SUPPLEMENTARY TEXT
Positive Regulatory Dynamics by DsrA noncoding RNA

Raúl Guantes[1], Bastien Cayrol[2,3], Florent Busi[4,5] and Veronique Arluison[2,3,4]

[1] Department of Condensed Matter Physics, Facultad de Ciencias, Universidad Autónoma de Madrid, Madrid, Spain, and Instituto 'Nicolás Cabrera', Facultad de Ciencias, Universidad Autónoma de Madrid, 28049 Madrid, Spain

[2] Laboratoire Léon Brillouin, Commissariat lEnergie Atomique, CNRS-UMR 12, CEA-Saclay, Gif-sur-Yvette Cedex F-91191

[3] Laboratoire Jean Perrin, FRE 3132 CNRS-Paris 6 Paris F-75006

[4] Universit Paris Diderot - Paris 7 Paris F-75013

[5] Unit de Biologie Fonctionnelle et Adaptative (BFA), CNRS EAC 4413, Universit Paris Diderot-Paris 7, Paris F-75013

1 Models of σ^S positive regulation by DsrA

We considered a simple rate equation model of *rpoS* activation by DsrA, similar to other existing models of negative regulation by sRNAs in bacteria [1–4] and miRNAs in mammalian cells [5]. In the first version of the model we take into account the dynamics of four molecular species: D(free DsrA), r(free *rpos* mRNA), c(rpos/DsrA complex) and R(RpoS or σ^S protein), which can change according to the following biochemical reactions:

1) Transcription of DsrA and *rpoS* RNAs:

$$\emptyset \quad \xrightarrow{\alpha_D} \quad D,$$
$$\emptyset \quad \xrightarrow{\alpha_r} \quad r,$$

(1.1)

where the transcription rates α_D and α_r are not known and should be fitted from the quantification data. Since DsrA transcription increases with temperature [6], we assume a general temperature dependence for DsrA transcription rate:

$$\alpha_D(T) = \frac{\alpha^0}{1 + (T/K_T)^{n_T}}$$

(1.2)

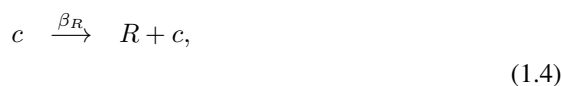This functional form seems appropriate in view of the quantification data for DsrA (see main text).

2) Association/dissociation of DsrA/rpos mRNA:

$$D + r \quad \xrightarrow{k_+} \quad c,$$

$$c \xrightarrow{k_-} D + r,$$

$$(1.3)$$
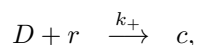
In previous modeling work it has been assumed that complex association and dissociation are fast reactions and thus in equilibrium with respect to transcription and degradation reactions. Recent *in vitro* studies by FRET of the annealing dynamics of DsrA and *rpoS* mediated by Hfq have shown that this is a sequential process involving binding to Hfq, unwinding of RNA and *rpoS* and annealing, with slow time scales for unwinding and annealing on Hfq of the order of minutes [7]. Therefore we take fully into account both reactions in our model. We note that fast equilibrium approximation does not affect steady state levels of the molecular species, but will change the response at short times.

4) RpoS translation from the active c complex, and degradation reactions.

$$c \xrightarrow{\beta_R} R + c,$$

$$(1.4)$$

$$D \xrightarrow{\delta_D} \emptyset,$$
$$r \xrightarrow{\delta_r} \emptyset,$$
$$c \xrightarrow{\delta_c} \emptyset,$$
$$P \xrightarrow{\delta_P} \emptyset,$$

$$(1.5)$$

The time evolution of the four molecular species is given by the set of ordinary differential equations:

$$\frac{dD}{dt} = \alpha_D(T) + k_- \cdot c - k_+ \cdot D \cdot r - \delta_D D + (1-p)\delta_c c, \qquad (1.6)$$

$$\frac{dr}{dt} = \alpha_r + k_- \cdot c - k_+ \cdot D \cdot r - \delta_r r, \qquad (1.7)$$

$$\frac{dc}{dt} = k_+ \cdot D \cdot r - k_- \cdot c - \delta_c c, \qquad (1.8)$$

$$\frac{dR}{dt} = \beta_R \cdot c - \delta_R R \qquad (1.9)$$

The parameter p takes into account the possibility of selective degradation of the sRNA/mRNA duplex [8],that is, p is the probability that degradation of the mRNA in the complex is accompanied by degradation of the sRNA. In the main text we use $p = 1$ (stoichiometric degradation of the duplex).

The steady state levels of the different species can be expressed in terms of the kinetic rates as

$$D^* = \frac{p}{2\delta_D} \left[\left(\frac{\alpha_D}{p} - \alpha_r - \lambda \right) + \sqrt{\left(\frac{\alpha_D}{p} - \alpha_r - \lambda \right)^2 + 4\lambda \frac{\alpha_D}{p}} \right], \quad (1.10)$$

$$r^* = \frac{1}{2\delta_r} \left[\left(\alpha_r - \frac{\alpha_D}{p} - \lambda \right) + \sqrt{\left(\alpha_r - \frac{\alpha_D}{p} - \lambda \right)^2 + 4\lambda\alpha_r} \right], \quad (1.11)$$

$$c^* = \frac{1}{2\delta_c} \left[\left(\alpha_r + \frac{\alpha_D}{p} + \lambda \right) - \sqrt{\left(\alpha_r - \frac{\alpha_D}{p} + \lambda \right)^2 + 4\lambda\frac{\alpha_D}{p}} \right] \quad (1.12)$$

where the asterisk denote steady states and

$$\lambda = \frac{\delta_r \delta_D}{pK}, \quad (1.13)$$

$$K = \frac{\delta_c k_+}{k_- + \delta_c} \quad (1.14)$$

can be understood as a 'leakage' rate giving total RNA turnover not due to duplex formation, and an effective complex association constant respectively [1]. Notice that from a fitting to steady state levels as in main text we can only estimate K, but not individual association/dissociation rates k_+/k_-.

It is interesting to compare the response of our DsrA/*rpoS* system to other cases of negative regulation by sRNAs, where a threshold-linear behavior is observed as a function of the target mRNA transcription rate for strong complex association(large K) [1, 5]. In our case, the response to temperature stress is dictated by the amount of active complex c. If $\lambda << 1$, Eq. (1.12) shows two well differentiated regimes:

1) For $\alpha_D < \alpha_r$ (DsrA transcription rate smaller than *rpoS* transcription), $c^* \simeq \alpha_D/\delta_c$, implying a linear increase of the active duplex with α_D (tuned by temperature).

2) For $\alpha_D > \alpha_r$, $c^* \simeq \alpha_r/\delta_c$, so that c^* level is constant (independent of α_D).

For smaller λ this linear-threshold behavior (opposite to sRNA repression) will be smoothened. We show this in Figure S2A, where all the parameters have been fixed to the experimentally obtained values (Table 2 in main text) except K, which is allowed to change in the range $[0.1, 1000]$, and the DsrA transcription rate α_D. Production of the active complex c^* for the values of K and α_D obtained from the fitting to experimental data (with α_D dependent on temperature in the range $T \in [10, 42]°C$) is shown with dashed lines. We see that σ^S induction *in vivo* lies in an intermediate regime with approximately linear increase in c^* production far from saturation. This is because the threshold for saturation is set by *rpoS* transcription rate (α_r) which is larger than α_D and never reached in physiological conditions.

This fact also allows the system to be sensitive to changes in temperature. The sensitivity can be defined as the logarithmic gain of the product with respect to the input. We thus take as product the concentration of active complex, c^*, and as input the (temperature dependent) DsrA transcription rate, so that $sensitivity = d\log c^*/d\log \alpha_D$ [1,9]. In Figure S2B we plot the sensitivity for the same K values as in Figure S2A. We note that, in stark contrast to other systems with mRNAs acting as postranscriptional repressors [1], where sensitivity in the target mRNA can be $>> 1$ at the threshold, in post-transcriptional activation the maximum gain for the *active* complex is limited to 1 (achieved in the linear regime below threshold, which can be seen taking derivatives from Eq.(1.12)). In spite of this smaller sensitivity for positive regulatory dynamics, physiological conditions keep the system in the regime with relatively high sensitivity (dashed line in Figure S2B).

1.1 Model with DsrA oligomer formation.

Taking into account the possibility that free DsrA monomers can associate to form oligomers, we must include oligomer association/dissociation reactions

$$
\begin{aligned}
nD & \xrightarrow{k_a} D_n, \\
D_n & \xrightarrow{k_d} nD.
\end{aligned}
\tag{1.15}
$$

Then we have a new variable, D_n, which is the oligomer concentration, and Eqs. (1.6-1.9) now read:

$$
\frac{dD}{dt} = \alpha_D(T) + k_- c + n k_d D_n - k_+ D \cdot r - k_a D^n - \delta_D D, \tag{1.16}
$$

$$
\frac{dD_n}{dt} = k_a D^n - k_d D_n - \delta_o D_n, \tag{1.17}
$$

$$
\frac{dr}{dt} = \alpha_r + k_- c - k_+ D \cdot r - \delta_r r, \tag{1.18}
$$

$$
\frac{dc}{dt} = k_+ D \cdot r - k_- c - \delta_c c, \tag{1.19}
$$

$$
\frac{dR}{dt} = \beta_R \cdot c - \delta_R R \tag{1.20}
$$

Eqns. (1.18-1.20) are the same as the previous Eqs. (1.7-1.9), since we assume that only DsrA monomers form heteroduplex with *rpoS* to initiate RpoS transcription. Oligomers can be degraded independently from monomers (with rate δ_o) [10]. The steady-state values of the different molecular species depend on the same parameters used for the simplified model in Eqs. (1.6-1.9), and three new parameters: the oligomer degradation rate δ_o, the oligomer length n, and the net oligomer association rate defined in analogy to Eq. (1.14),

$$
K_o = \frac{\delta_o k_a}{k_d + \delta_o} \tag{1.21}
$$

Steady state solutions for free DsrA and *rpoS* can be found solving the following equations:

$$
\begin{aligned}
\alpha_D(T) - KD \cdot r - n K_o D^n - \delta_D D &= 0, \tag{1.22} \\
\alpha_r - KD \cdot r - \delta_r r &= 0 \tag{1.23}
\end{aligned}
$$

which are similar to the steady state equations in the case that DsrA is only in monomeric form except for the 'non-linear degradation' term $n K_o D^n$. Solution of Eqs. (1.22-1.23) is not analytic for a general value of n, so we solve them numerically to find the steady-state levels of all the molecular species. Since we checked that polymers could be detected by our RT-qPCR assay(see main text), the quantities fitted to experimental points are now the total amounts of *rpoS* and DsrA including polymer,

$$
\begin{aligned}
D_t &= D + n D_n + c, \\
r_t &= r + c,
\end{aligned}
\tag{1.24}
$$

4

As expected from the low levels of total DsrA measured in cells, we found that for compatibility of fitting with known parameters and quantification data, two conditions should be met: first, that polymer halflife should be much shorter than monomer halflife, as it was found experimentally *in vitro* in Ref. [10]. Second, only oligomers with low copy number (dimers-tetramers at most) were able to reasonably fit quantification data.

2 Role of duplex reversibility in response dynamics.

For duplex association mediated by Hfq, our only experimentally accessible parameter is the effective association constant K given by Eq. (1.14). Individual association and dissociation constants, k_+/k_-, cannot be uniquely determined but are interdependent. For the experimentally fitted value of K (Table 2 in main text), we vary the dissociation constant k_- in a wide range and calculate the corresponding k_+ value (Figure S3A). We distinguish two regimes: one where the association rate constant is much larger than the dissociation ($k_+ > 100k_-$, left of the dashed blue line in Figure S3A), so that the duplex is essentially irreversible at any DsrA concentration, and a regime where $k_- > k_+$ (right of dashed red line in Figure S3A), and thus duplex formation can be considered a reversible process. In this last case the dissociation rate should be $k_- > 10\,\text{h}^{-1}$. When applying the same criterium for different values of the effective constant K, we find that for $K \gtrsim 14\,\text{nM}^{-1}.\text{h}^{-1}$ there is no reversible regime in the k_- range studied.

To study the influence of reversibility on the dynamics, we calculate the activation and deactivation times for the σ^S protein as a function of the temperature change (as in Figure 4 in main text), for a large range of the complex dissociation constant. The activation and recovery times are plotted as color maps in Figure S3B and S3C respectively. We see that in the whole irreversible regime dynamics is unaffected by the particular value of k_-, but both activation and recovery times become slightly faster in the reversible regime ($k_- > 10$).

3 Noise analysis of σ^S induction by DsrA

We calculated intrinsic noise in steady-state levels of active DsrA/*rpoS* complex and σ^S protein using both exact stochastic simulation of all the biochemical reactions involved with a Monte Carlo algorithm [11], and a linear noise approximation for the dynamics [12]. The linear noise approximation gives the covariance matrix of the fluctuations around steady states by solving the algebraic Lyapunov equation:

$$\boldsymbol{M} \cdot \boldsymbol{\sigma} + \boldsymbol{\sigma} \cdot \boldsymbol{M^T} + \boldsymbol{D} = \boldsymbol{0}, \qquad (3.25)$$

where $\boldsymbol{M}$ is the normalized Jacobian matrix, whose elements are defined as [12]

$$M_{ij} = \frac{\bar{n}_j}{\bar{n}_i}\left(\frac{\partial \bar{J}_i^+}{\partial \bar{n}_j} - \frac{\partial \bar{J}_i^-}{\partial \bar{n}_j}\right), \qquad (3.26)$$

with $\bar{n}_i$ the macroscopic concentration of the ith molecular species at equilibrium and $\bar{J}_i^-/\bar{J}_i^+$ the total degradation and synthesis rates at equilibrium. $\boldsymbol{\sigma}$ is the matrix of normalized covariances, $\sigma_{ij} = \langle(n_i - \bar{n}_j)(n_j - \bar{n}_j)\rangle/\bar{n}_i\bar{n}_j$ (note that σ_{ii} is the squared coefficient of variation for fluctuations of the i component), and $\boldsymbol{D}$ the diffusion matrix

whose elements depend on the reaction fluxes, system size and stoichiometric coefficients [12, 13]. We can obtain the Jacobian matrix Eq. (3.26) and the diffusion matrix readily from the mass action law equations (1.9) and reactions (1.1,1.3-1.5). Then the Lyapunov equation (3.25) is numerically solved using subroutine *lyap* in MATLAB, MathWorks. We note that, contrary to simple models of gene expression or regulation by transcription factors [12, 14], the diffusion matrix is not diagonal due the coupling between DsrA and *rpoS* to form the duplex, and Eq. (3.25) has not direct analytic solution. However, if $DsrA$ and $rpoS$ fluctuations can be approximately assumed as decoupled, as suggested by Figure 5B in main text, and noise in σ^S protein is only affected by the propagation of fluctuations in the active duplex, we may consider Eq. (3.25) as effectively two-dimensional (taking into account only duplex and protein fluctuations) with diagonal diffusion matrix, which can be easily solved [13] and gives protein noise by Eq. (5) in main text.

The linear noise approximation has the advantage that noise amplitudes can be computed very efficiently, although it is in principle restricted to small size fluctuations. We have however found an excellent agreement between our numerical simulations and the result of the linear noise approximation in our system, for the whole physiological range of temperature variation (Figure 5 in main text). We thus use this approximation to systematically explore the role that the dissociation constant plays on the intrinsic noise (as in the previous section for the response times).

Consistent with the results of the previous section and the approximate Eq. (5) in main text, we see in Figure S4 that noise (both coefficient of variation and Fano factor) is unaffected by the value of the dissociation constant as long as the duplex is irreversible. For large values of k_-, however, the duplex becomes reversible and correlations between DsrA and *rpoS* fluctuations start to be significant, decreasing noise in protein production. A similar effect of correlations between molecular species has been observed in the context of signal detection by simple biochemical networks [15].

References

[1] Levine E, Zhang Z, Kuhlman T, Hwa T: **Quantitative characteristics of gene regulation by small RNA.** *PLoS Biol* 2007, **5**(9):e229.

[2] Mitarai N, Benjamin JAM, Krishna S, Semsey S, Csiszovszki Z, Massé E, Sneppen K: **Dynamic features of gene expression control by small regulatory RNAs.** *Proc Natl Acad Sci U S A* 2009, **106**(26):10655–9.

[3] Mehta P, Goyal S, Wingreen NS: **A quantitative comparison of sRNA-based and protein-based gene regulation.** *Mol Syst Biol* 2008, **4**:221.

[4] Legewie S, Dienst D, Wilde A, Herzel H, Axmann IM: **Small RNAs establish delays and temporal thresholds in gene expression.** *Biophys J* 2008, **95**(7):3232–8.

[5] Mukherji S, Ebert MS, Zheng GXY, Tsang JS, Sharp PA, van Oudenaarden A: **MicroRNAs can generate thresholds in target gene expression.** *Nat Genet* 2011, **43**(9):854–9.

[6] Repoila F, Gottesman S: **Signal transduction cascade for regulation of RpoS: temperature regulation of DsrA.** *J Bacteriol* 2001, **183**(13):4012–23.

[7] Hwang W, Arluison V, Hohng S: **Dynamic competition of DsrA and rpoS fragments for the proximal binding site of Hfq as a means for efficient annealing.** *Nucleic Acids Res* 2011, **39**(12):5131–9.

[8] Hao Y, Xu L, Shi H: **Theoretical analysis of catalytic-sRNA-mediated gene silencing.** *J Mol Biol* 2011, **406**:195–204.

[9] Buchler NE, Louis M: **Molecular titration and ultrasensitivity in regulatory networks.** *J Mol Biol* 2008, **384**(5):1106–19.

[10] Cayrol B, Geinguenaud F, Lacoste J, Busi F, Le DÃrout J, Pietrement O, Le Cam E, Regnier P, Lavelle C, Arluison V: **Auto-assembly of E. coli DsrA small non-coding RNA: Molecular characteristics and functional consequences.** *RNA Biol* 2009, **6**(4):434–45.

[11] Gillespie DT: **Exact Stochastic Simulations of Coupled Chemical Reactions**. *Journal of Phys Chem* 1977, **81**:2340–60.

[12] Paulsson J: **Models of Stochastic Gene Expression**. *Physics of Life Reviews* 2005, **2**:157–75.

[13] Paulsson J: **Summing up the noise in gene networks.** *Nature* 2004, **427**(6973):415–8.

[14] Guantes R, Estrada J, Poyatos JF: **Trade-offs and noise tolerance in signal detection by genetic circuits.** *PLoS One* 2010, **5**(8):e12314.

[15] Tanase-Nicola S, Warren PB, ten Wolde PR: **Signal detection, modularity, and the correlation between extrinsic and intrinsic noise in biochemical networks.** *Phys Rev Lett* 2006, **97**(6):068102.
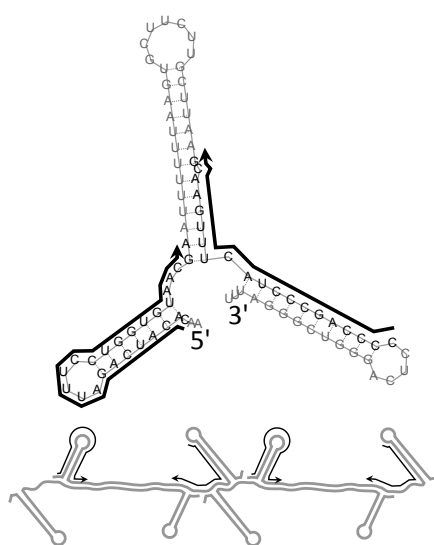
Fig. S1: Hybridization region of the oligonucleotides used for the quantification of DsrA. Oligonucleotides for reverse transcription and amplification (black arrows) were chosen in order to amplify most of the DsrA cDNA sequence, to prevent the formation of primer dimers (top) and to avoid as much as possible the priming in the polymerization region (bottom). (RNA structures were derived from RNAfold web server predictions, http://rna.tbi.univie.ac.at/cgi-bin/RNAfold.cgi; computer-predicted structure may differ with nuclease footprint structures).
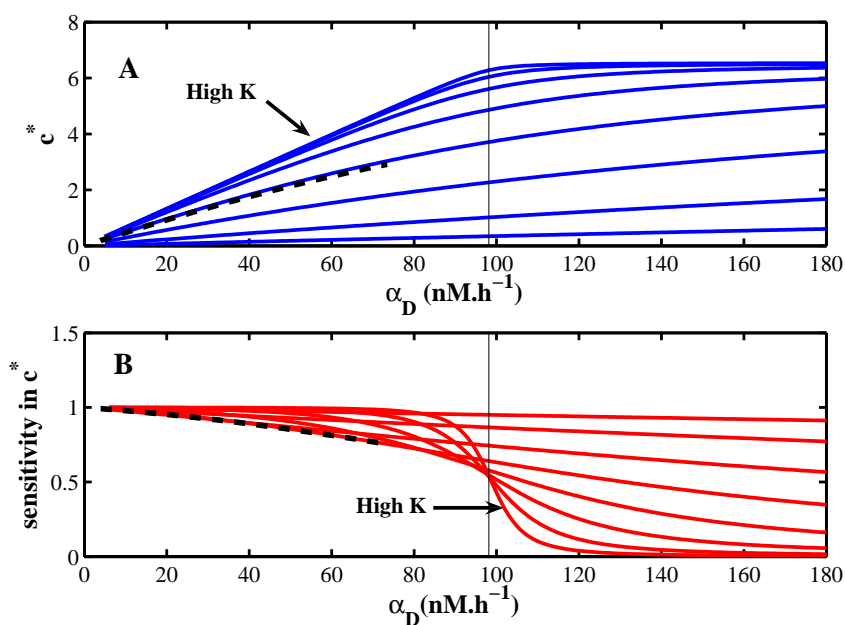
Fig. S2: Response properties of the DsrA/*rpoS* system as a function of the DsrA transcription rate for different values of the effective duplex association constant K (see text). The values of the rest of the parameters are taken from the experimental fits. Vertical thin lines mark the value of the *rpoS* transcription rate (Table 2). Dashed lines show the behavior given for the experimentally fitted values of K and α_D, in a temperature range $T \in [10, 42]°C$. A. Steady state levels of the active DsrA/*rpoS* duplex as a function of DsrA transcription rate(which in turn is modulated by temperature) for different values of the effective complex association constant K. Dashed lines: Active duplex levels for the experimentally fitted values of K and α_D in the temperature range $[10, 42]°$. B. Sensitivity of the active complex as a function of DsrA transcription rate for the same K values as in panel A.
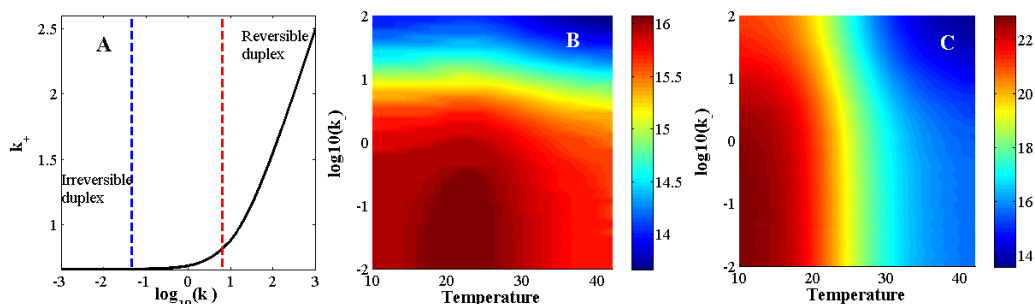
Fig. S3: **Role of duplex reversibility in response times**. A. Duplex association constant as a function of dissociation rate, for a value of the effective association constant $K = 4.6$ nM^{-1}.h^{-1} (fitted to experiments). Dashed blue line marks the limit where $k_+ \geq 100k_-$. Red line denotes the limit of $k_- > k_+$. B. σ^S activation time as a function of temperature and dissociation constant. C. σ^S recovery time as a function of temperature and dissociation constant.
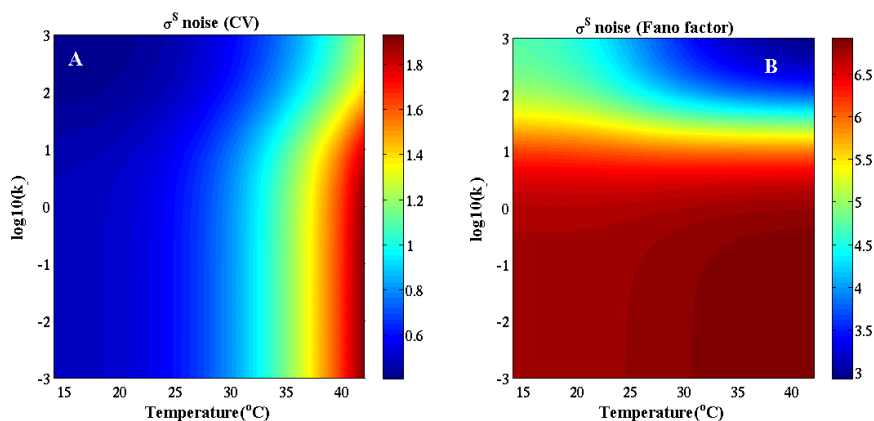

Fig. S4: **Role of duplex reversibility on intrinsic noise**. A. Noise coefficient of variation for σ^S protein as a function of temperature and complex dissociation constant k_-. B. Fano factor as a function of temperature and k_-. Degradation of DsrA is considered independent of temperature, but qualitatively a similar behavior is observed for a temperature dependent degradation rate, with the exception that noise increases at high temperatures (see Figure 5A in main text).

10